

# Reliability Analyses of Wide-Area Protection System Considering Cyber-Physical System Constraints

Ruiwen He<sup>1</sup>, Senior Member, IEEE, Shenghui Yang, Jianhua Deng, Teng Feng, Loi Lei Lai, Fellow, IEEE, and Mohammad Shahidepour<sup>2</sup>, Life Fellow, IEEE

**Abstract**—Wide-area measurement, protection and control systems link the cyber power system with the physical power system to realize a cyber-physical power system (CPPS). This paper proposes a reliability modeling and assessment method for the wide-area protection system (WAPS). The proposed WAPS model takes into account the decision accuracy of protection algorithms with limited available data at the control center, and combines it with the tripping reliability of protection devices in corresponding substations to form the operation accuracy of WAPS. In particular, the directional comparison algorithm used in decision-making is functionally divided into three modules, namely the initiation module, the fault area positioning module, and the faulted element recognition module. The proposed reliability models are established based on the Permutation and Combination method under the assumption that the data acceptance rate of the control center is  $d$ . The sequential Monte-Carlo simulation is used to solve the proposed reliability indices. Finally, the WAPS reliability assessment is presented for the IEEE 14-bus system and the key influencing factors are identified and discussed.

**Index Terms**—Cyber-physical power system (CPPS), data flow, protection algorithm, reliability analysis, wide-area protection system (WAPS).

Manuscript received October 14, 2020; revised January 6, 2021 and February 2, 2021; accepted February 17, 2021. Date of publication February 19, 2021; date of current version June 21, 2021. This work was supported in part by the National Natural Science Foundation of China under Grant 51377026; in part by Laboratory Construction Project of Intelligent Substation Design and Simulation of State Grid Economic and Technological Research Institute of China under Grant Q14415190002; and in part by the Department of Finance and Education of Guangdong Province under Grant 2016[202]: Key Discipline Construction Programme, China. Paper no. TSG-01532-2020. (Corresponding author: Loi Lei Lai.)

Ruiwen He, Shenghui Yang, and Loi Lei Lai are with the Department of Electrical Engineering, School of Automation, Guangdong University of Technology, Guangzhou 510006, China.

Jianhua Deng is with the Foshan Electric Power Company Ltd. China, Southern Power Grid, Foshan 528000, China.

Teng Feng is with the Automation and Control Design Research Center, State Grid Economic and Technological Research Institute Company Ltd., Beijing 102209, China.

Mohammad Shahidepour is with the Electrical and Computer Engineering Department, Illinois Institute of Technology, Chicago, IL 60616 USA, and also with the ECE Department, King Abdulaziz University, Jeddah 21589, Saudi Arabia (e-mail: ms@iit.edu).

Color versions of one or more figures in this article are available at <https://doi.org/10.1109/TSG.2021.3060941>.

Digital Object Identifier 10.1109/TSG.2021.3060941

## I. INTRODUCTION

WITH the continuously increasing deployment of variable energy sources and flexible loads, the uncertainty and the complexity of instantaneously balancing the energy flows in power grids are also rising. The efficiency, sustainability, reliability, and security of power systems will progressively depend on the support of information technology to regulate the energy flow via the information flow. The coupling of information and energy flows will lead to the development of cyber-physical power system (CPPS) [1]–[2].

Considering the expansion in the deployment of cyber infrastructure, the reliability of CPPS is worthy of further investigation. The conventional power system reliability mainly focuses on the failure of physical system components, in which cyber element functionalities are considered perfectly reliable. In CPPS, the reliable operation of a power system depends highly on the situational awareness in the information system.

CPPS promotes certain wide-area applications for measurement and control including the wide-area measurement system (WAMS) and the wide-area protection system (WAPS) [3], [4]. Different from traditional relay protection systems, which use the local information for decision-making, the WAPS accuracy in recognizing and isolating faults is inseparable from the effectiveness of WAMS, which is distributed in large geographical areas.

The WAPS decision model can adopt either a centralized or a distributed layout. The distributed layout allocates the decision-making process to intelligent electronic devices (IEDs) in each substation. The IEDs perform intelligent analysis by collecting the data from adjacent substations [5], [6]. The philosophy of protection schemes based on the centralized concept constructed on WAMS can resolve many of the protection limitations [7]. The centralized layout sets up a control center in the master station to collect the regional power grid data. The control center analyzes the collected data, makes decisions, and sends control commands to substation IEDs for clearing the faulted elements. The WAPS algorithm plays a key role in the decision-making process. In the smart grid where data sharing is encouraged, WAPS can adopt pilot scheme, whose mature algorithms are divided into two categories. One uses the current differential protection principle [8]–[10], and the other

applies the directional comparison protection principle [11]–[13]. The latter is easier to implement because it does not strictly require wide-area data synchronization.

The WAPS reliability hinges on the topology connectivity of the wide-area network (WAN) which feeds the uploaded WAMS data to control centers. The research on WAPS reliability, especially that on network connectivity, has made significant achievements [14]–[16]. However, network imperfections are critical for control performance and even the stability of wide-area power systems [17]. Communication reliability also concerns data timeliness, data availability, and data accuracy [18], especially the delays associated with data and command communications and algorithm executions can be a troublesome issue in a large-scale power system [19].

Considering the WAPS dependence on the wide-area information flow for its operation, the protection system may have functional failures because of the incomplete information and the degradation in WAMS performance. Hence, it is obvious that the implementation of the protection function is limited not only by the topological connectivity of associated physical components, but also by the information system performance. Reference [20] analyzed the operating characteristics of differential protections under normal conditions, external and internal faults of a transformer, while packet loss/delay occurs at different times and using different corrective measures. It is considered that the impact of the packet delay is equivalent to the packet loss for a protection algorithm. Reference [21] stated that the general binary-state description of each component cannot identify the deterioration degree of the information performance. The study introduced the stochastic-flow network (SFN) to model flow-limited protection systems, and formed a practicable reliability assessment approach. Reference [22] studied the reliability of cyber space at the  $d$ -level under degradation and even congestion circumstances, which means the maximum network flow is not less than  $d$  units by the sink. It is expressed by the composite Markov process using the Monte-Carlo simulation and the maximum-flow technique.

In this paper, we study the WAPS reliability embodying the information flow at  $d$ -level. The proposed idea suggests for the first time a new method to associate WAPS algorithms with the  $d$ -level data, and two indices to measure reliability in terms of decision and operation accuracies. Based on the specific WAPS arrangement and algorithm, such as centralized layout and directional comparison algorithm, we decompose the protection functional modules and establish the probability models so that each module can be correctly implemented under a given  $d$  by using Permutation and Combination. We combine the decision accuracy of protection algorithms at  $d$ -level with the tripping reliability of protection devices in physical substations to substantiate the operation accuracy of WAPS.

We studied the reliability of cyber space at the  $d$ -level in our previous paper [22], considering that WAPS in smart grid links the power information system with the physical power system to realize a closed-loop. In this paper, we further associate the WAPS algorithm with the information flow at  $d$ -level. Thus, we have implemented a new CPPS

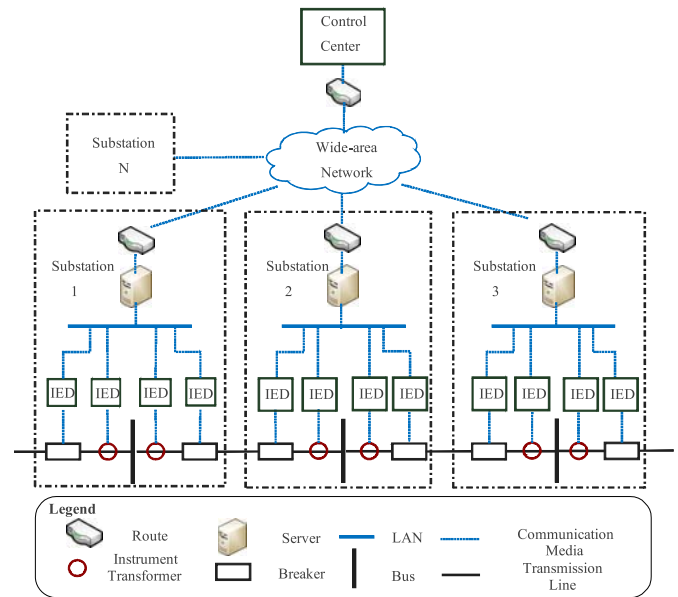


Fig. 1. WAPS with centralized decision-area model.

reliability analysis methodology, in which WAPS is regarded as a middleware, and a series of innovative ideas and research methods are organically combined including stochastic-flow network model, composite Markov model, maximum-flow technique, linear programming model, permutation and combination, sequential Monte-Carlo simulation, decision accuracy, and operation accuracy of WAPS.

The remainder of this paper is organized as follows. Section II proposes the general reliability analysis model for the regional centralized WAPS arrangement. Section III establishes the reliability model of WAPS decision-making process under the condition that the data acceptance rate by the control center is  $d$ , in which the directional comparison scheme is adopted. Section IV gives the reliability model of WAPS tripping process in corresponding substations. Also, it presents the definition of reliability indices and the computation procedure using the sequential Monte-Carlo simulation. Section V implements the proposed reliability assessment methodology to the case study based on the IEEE 14-bus system, and analyzes the key influence factors on the WAPS reliability. Section VI concludes the paper.

## II. FRAMEWORK FOR WAPS RELIABILITY MODEL

In this paper, we apply a centralized decision model for reliability analyses. The centralized layout adopted in this paper is shown in Fig. 1. The substation IEDs are responsible for data collection including analog quantities and switching values. The collected data are integrated with a substation server through a local area network (LAN) in the substation and uploaded to the master station in the control center through a WAN. Furthermore, the control center recognizes faulted elements by analyzing the data collected and generates a trip signal as decision, which is sent to substation IEDs for implementation.

WAPS in this paper is expressed as a CPPS. In cyber space, WAPS includes data acquisition, transmission, and utilization for issuing protection and control commands. WAPS cyber decision process includes uploading the WAMS data from substations, data transmission within WAN to the control center, the faulted element recognition in the control center and the submission of trip commands to IEDs, while considering communication network constraints. Whereas, WAPS physical part mainly refers to maintaining the relay protection units in working state. Obviously, only when the cyber and physical layouts of WAPS are considered reliable and can work in tandem, then the fault location can be identified and the protection device can perform correctly, and faulted elements can be effectively removed and isolated.

Accordingly, the operation accuracy  $P_{act}$  is used to reflect the WAPS reliability in the regional power grid when a fault occurs. The uploading of data to WAN at each substation and the relay protection operation is described by stationary stochastic processes  $X(t)$ ,  $Y(t)$ , respectively, where  $t \in \mathbb{R}^+$ . The sample space of  $X(t)$  is a set of positive real numbers  $\mathbb{R}^+$  and the sample space of  $Y(t)$  is  $\{0, 1\}$ , in which only normal (functional) and failure states exist. Suppose there are  $n$  substations equipped with WAPS in the regional power grid, where a substation is denoted as a node. Set  $\mathbb{X} = \{X_1(t), \dots, X_n(t)\}$  to represent the WAMS measurement data flow uploading process at each node. Likewise,  $\mathbb{Y} = \{Y_1(t), \dots, Y_n(t)\}$  characterizes the relay protection operation process at each node. Let  $m_{xi}(t) := EX_i(t) = \int_{-\infty}^{+\infty} x_i dF_i(x_i; t)$  be the expectation of the uploaded data flow at node  $i$ , where  $F_i$  is a distribution function of the stochastic process  $X_i(t)$ ; then the expectation of the total uploaded data flow in the regional grid is stated as follows:

$$\bar{\Gamma} := \sum_{i=1}^n m_{xi}(t) \quad (1)$$

Similarly, let  $m_{yi}(t) := EY_i(t) = \int_{-\infty}^{+\infty} y_i dG_i(y_i; t)$  be the expectation of the relay protection operation process at node  $i$ , where  $G_i$  is the distribution function of the stochastic process  $Y_i(t)$ , and the steady-state probability of the protection process in normal state at substation  $i$  is obtained by

$$p_{i.pro} := 1 - m_{yi}(t) \quad (2)$$

The uploaded data flow at the substations must pass through a constrained WAN to reach the control center in the master station. Assume  $\mathcal{W}$  is a function representing the uploaded data flow constraint within WAN's limited bandwidth. Let  $\bar{\Psi} := \mathcal{W}(M_x)$  be the expectation of the maximum data flow received at the master station, where  $M_x = \{m_{x1}, \dots, m_{xn}\}$  represents the average flow injected into WAN from each node; then the expected data flow acceptance rate at the control center is:

$$\bar{d} = \bar{\Psi} / \bar{\Gamma} \quad (3)$$

This indicator reflects that only  $\bar{d}\%$  of the WAMS measured data can be uploaded to the control center due to the limited WAN bandwidth allocation to the communication network. However, the WAPS algorithm at the control center cannot

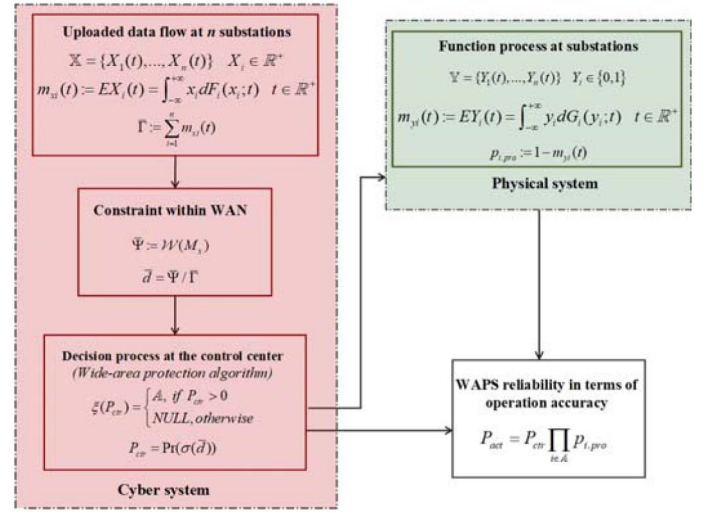


Fig. 2. Framework for WAPS reliability analysis.

guarantee to recognize the faulted element reliably using the  $\bar{d}\%$  available data. Thus, the WAPS probability to recognize the fault and generate a trip command is a decision accuracy term defined as  $P_{ctr}$ :

$$P_{ctr} = \Pr(\sigma(\bar{d})) \quad (4)$$

where function  $\sigma$  represents the adopted WAPS algorithm (e.g., wide-area directional comparison algorithm, wide-area current differential algorithm). When the fault can be recognized with a certain probability, the control center can simultaneously return the functional set of actions to substations as:

$$\xi(P_{ctr}) = \begin{cases} \mathbb{A}, & \text{if } P_{ctr} > 0 \\ \text{NULL}, & \text{otherwise} \end{cases} \quad (5)$$

where, a control command is sent to the substations in set  $\mathbb{A}$ . If the relay protection operation probability in substation  $i$  is  $p_{i.pro}$ , where  $i \in \mathbb{A}$ , the expectation of the WAPS operation is calculated as:

$$P_{act} = P_{ctr} \prod_{i \in \mathbb{A}} p_{i.pro} \quad (6)$$

The WAPS reliability in the regional power grid is accordingly stated by  $P_{act}$ . The framework for WAPS reliability analysis is shown in Fig. 2.

### III. RELIABILITY MODELING OF WAPS DECISION PROCESS

Suppose that the current WAN operation state is  $\mathbf{T}$ .  $\Gamma$  and  $\Psi$  represent the data flow uploaded by all acquisition nodes and the maximum flow received at the control center in state  $\mathbf{T}$ , respectively. And  $d \in [0, 1]$  indicates the data flow acceptance rate at the control center, which is expressed as  $d = \Psi / \Gamma$ . Apparently, a higher acceptance rate corresponds to a higher WAN performance. The reliability model of the WAPS decision-making process is proposed when the WAN is in state  $\mathbf{T}$  (i.e., control center can only receive  $d\%$  of the

acquisition data). Next, we determine the probability of a correct decision by control center for a limited WAN data when a fault occurs in the regional power grid.

In this paper, we adopt the directional comparison algorithm in the decision process to establish the WAPS reliability model. We functionally divided it into the following three modules, that is, an initiation module  $h(\mathbb{U}_{(1)})$ , a fault area positioning module  $\varpi(\mathbb{U}_{(1)})$ , and a faulted element recognition module  $\eta(\Phi)$ . For simplicity, the faulted element in this paper is a transmission line with a three-phase short-circuit fault. These three modules are discussed as follows.

#### A. Reliability Model for Protection Initiation Module

When a transmission fault occurs, the sequence of voltage yields significant characteristics. The closer to the fault location, the lower the positive sequence voltage is, and the larger the negative and the zero sequence voltages are at each bus. It is assumed that the positive sequence voltage is used as an initial reference for WAPS. Of course, the same analysis can be done by using other reference quantities.

Suppose that a set of the original sequence voltages uploaded by substations is  $\mathbb{U}_{(1)}^0 = \{U_1, U_2, \dots, U_n\}$ . The set of sequence voltages received by the control center is  $\mathbb{U}_{(1)} \subseteq \mathbb{U}_{(1)}^0$ , and supposed that the loss probability of these sequence voltages passing through a limited network is equal. The initiation setting value of the sequence voltage in the control center is  $U_{set}$ . The protection initiation determination function is expressed as

$$h(\mathbb{U}_{(1)}) = \begin{cases} 1, & |\min\{\mathbb{U}_{(1)}\}| \leq U_{set} \\ 0, & \text{otherwise} \end{cases} \quad (7)$$

In fact, any power system fault may cause sequence voltage of at least one bus to meet the initiation condition. Function  $h(\mathbb{U}_{(1)})$  indicates that the WAPS process will be initiated when any bus sequence voltage in set  $\mathbb{U}_{(1)}^0$  is less than the preset initiation setting value. Accordingly, when WAN is in state  $\mathbf{T}$  for a given  $d$ , the probability of accurately initiating WAPS using Permutation and Combination is stated as:

$$P_{sf} = \begin{cases} 0, & S = 0 \\ \frac{\sum_{i=1}^{\Upsilon\delta} C_{S^0-i}^{S-1}}{C_{S^0}^S}, & 0 < S < S^0 - \Upsilon\delta + 1 \\ 1, & S^0 - \Upsilon\delta + 1 \leq S \leq S^0 \end{cases} \quad (8)$$

where  $S^0 = \delta \text{card}(\mathbb{U}_{(1)}^0)$  is the bus sequence voltage data uploaded by substations;  $\delta$  is the data redundancy;  $\text{card}(\bullet)$  describes the set cardinality;  $S = \lfloor S^0 d \rfloor$  is the data flow received by the control center at a given  $d$ , where  $S \in \mathbb{N}$  and  $S \propto d$ ; the floor function is shown by  $\lfloor \cdot \rfloor$ ;  $\Upsilon$  is the total number of buses which meet the initiation setting value of sequence voltage when a fault occurs;  $C_n^k$  is the number of  $k$ -combinations for a given set of  $n$  elements.

The derivation of (8) in using Permutation and Combination is given below. If  $S = 0$ , it is obvious that no fault related information can be obtained; so the probability of accurately initiating WAPS is 0. And if  $0 < S < S^0 - \Upsilon\delta + 1$ , the WAPS process will be initiated when any bus sequence voltage is less than the preset initiation setting value. When a bus

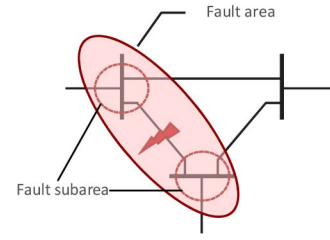


Fig. 3. Schematic diagram of a fault area.

sequence voltage which satisfies the conditions is taken out, the number of events containing this bus sequence voltage is  $C_{S^0-1}^{S-1}$ ; when the next bus sequence voltage which satisfies the conditions is taken out, the number of events containing this bus sequence voltage and excluding the bus sequence voltage previously taken is  $C_{S^0-2}^{S-1}$ , and so on. We continue this process until all bus sequence voltages which satisfy the conditions are taken out, where the sum shows the number of events in which at least one bus sequence voltage is less than the initiation setting value in terms of  $\sum_{i=1}^{\Upsilon\delta} C_{S^0-i}^{S-1}$ . The number of elementary events receiving  $S$  bus sequence voltages is  $C_{S^0}^S$ . Therefore, the probability of accurately initiating WAPS is  $\frac{\sum_{i=1}^{\Upsilon\delta} C_{S^0-i}^{S-1}}{C_{S^0}^S}$ . Then  $S^0 - \Upsilon\delta + 1 \leq S \leq S^0$ , where it is apparent that at least one bus sequence voltage satisfying the conditions must be received; so the probability of accurately initiating WAPS is 1.

#### B. Reliability Model for Fault Area Positioning Module

After the protection was successfully initiated, the initial fault area can be reduced by certain rules which resort to power direction angle. In Fig. 3, the fault area  $\Lambda$  consists of several fault subareas. The fault subarea  $\Lambda_i$  in this case consists of bus  $i$  and all its outgoing lines.

Once a bus sequence voltage is detected to be less than the initiation setting value, the bus area is considered as a fault area.

Accordingly, the fault area positioning function is given as

$$\varpi(\mathbb{U}_{(1)}) = \begin{cases} \Lambda, & h = 1 \\ \text{NULL}, & \text{otherwise} \end{cases} \quad (9)$$

where  $\Lambda = \{\mathbb{L}, \mathbb{B}\} = \bigcup_{i=1}^{\Upsilon} \Lambda_i$ ;  $\mathbb{L}$  and  $\mathbb{B}$  are sets of transmission lines and buses in the fault area, respectively; and bus sequence voltages in area  $\Lambda$  satisfy  $|U_i| \leq U_{set}$ .

If the data acceptance rate is  $d$ , there is a chance that we would skip some of the existing faulted lines in the area located by (9). On the premise of successful protection initiation, we introduce the following rule for the accuracy of fault area positioning by applying the combination principle. Equation (10) indicates that the positioning can successfully identify a faulted line if the bus sequence voltage data are attainable by the control center for at least one of the two ends of a faulted line.

$$P_{fz} = \begin{cases} 0, & S = 0 \\ \frac{\sum_{i=1}^{\alpha\delta} C_{S^0-i}^{S-1}}{\sum_{i=1}^{\Upsilon\delta} C_{S^0-i}^{S-1}}, & 0 < S < S^0 - \alpha\delta + 1 \\ 1, & S^0 - \alpha\delta + 1 \leq S \leq S^0 \end{cases} \quad (10)$$

where  $\alpha \in \{1, 2\}$  represents the number of bus sequence voltage on the sending or the receiving end of a transmission line which satisfies the initiation criteria.

The derivation of (10) in using Permutation and Combination is given below. If  $S = 0$ , it is obvious that no fault related information can be obtained; so the probability of accurately positioning the fault area is 0. And if  $0 < S < S^0 - \alpha\delta + 1$ , the fault area will be positioned when any bus sequence voltage of two ends is less than the setting value. When a bus sequence voltage satisfying the conditions is taken out, the number of events containing this bus sequence voltage is  $C_{S^0-1}^{S-1}$ ; when the next bus sequence voltage satisfying the conditions is taken out, the number of events containing this bus sequence voltage and excluding the bus sequence voltage previously taken is  $C_{S^0-2}^{S-1}$ , and so on. We continue this process until all the bus sequence voltages meeting the conditions are taken out, where the sum shows the number of events that at least one bus sequence voltage is less than the initiation setting value in terms of  $\sum_{i=1}^{\alpha\delta} C_{S^0-i}^{S-1}$ . The number of elementary events accurately initiating WAPS is  $\sum_{i=1}^{\gamma\delta} C_{S^0-i}^{S-1}$ . Therefore, the probability of accurately positioning the fault area is  $\frac{\sum_{i=1}^{\alpha\delta} C_{S^0-i}^{S-1}}{\sum_{i=1}^{\gamma\delta} C_{S^0-i}^{S-1}}$ . Then  $S^0 - \alpha\delta + 1 \leq S \leq S^0$ , where it is apparent that at least one bus sequence voltage of two ends satisfying the conditions must be received; so the probability of accurately positioning the fault area is 1.

### C. Reliability Model of Faulted Line Recognition Module

After confirming the fault area  $\Lambda$ , it will be necessary to identify the faulted line in the area. According to the directional pilot relaying principle, when power directions at both ends of the line are positive, there is a fault between the two ends. Otherwise the fault is located outside. The criteria for the faulted line recognition is stated as

$$\eta(\Phi) = \begin{cases} L_i, & \text{if } [D(\varphi_{L_i}^+) \cap D(\varphi_{L_i}^-) = 1] \\ 0, & \text{otherwise} \end{cases}; L_i \in \Lambda \quad (11)$$

where,  $\varphi_{L_i}^+$ ,  $\varphi_{L_i}^-$  are sending and receiving end phase angles of line  $L_i$  respectively; the power direction discriminant is calculated as

$$D(\varphi) = \begin{cases} 1, & \text{if } \varphi \in (90^\circ, 270^\circ] \\ 0, & \text{if } \varphi \in (-90^\circ, 90^\circ] \end{cases} \quad (12)$$

where the phase angle is calculated as  $\varphi = \arg \frac{\dot{U}_{(1)}}{I_{(1)}Z_d}$ ;  $\dot{U}_{(1)}$  and  $\dot{I}_{(1)}$  are the positive sequence line voltage and current, respectively.  $Z_d$  is the line impedance. Of course, other types of directional elements can also be used, including those based on negative sequence, zero sequence, or variations of voltages and currents.

Similarly, if the current data acceptance rate of WAN is  $d$ , on the premise that the fault area is successfully located, the faulted line can be correctly identified as long as the direction angle data at both ends of the faulted line are not lost. The

accuracy of the faulted line recognition is given by

$$P_{fl} = \begin{cases} 0, & 0 \leq Q < 2 \\ 1 - \frac{2 \sum_{i=0}^Q C_\delta^i C_{Q^0-2\delta}^{Q-i} - C_{Q^0-2\delta}^Q}{C_{Q^0}^Q}, & 2 \leq Q < \delta \\ 1 - \frac{2 \sum_{i=0}^\delta C_\delta^i C_{Q^0-2\delta}^{Q-i} - C_{Q^0-2\delta}^Q}{C_{Q^0}^Q}, & \delta \leq Q \leq Q^0 - 2\delta \\ 1 - \frac{2 \sum_{i=\beta}^\delta C_\delta^i C_{Q^0-2\delta}^{Q-i}}{C_{Q^0}^Q}, & Q^0 - 2\delta < Q \leq Q^0 - \delta \\ 1, & Q^0 - \delta < Q \leq Q^0 \end{cases} \quad (13)$$

where  $Q^0 = 2\delta \text{card}(\mathbb{L})$  is the total amount of uploaded data of directional elements in area  $\Lambda$ ;  $\delta$  is the data redundancy;  $Q = \lfloor Q^0 d \rfloor$  is the amount of the direction data obtained by the control center; and  $\beta := Q - (Q^0 - 2\delta)$ .

The derivation of (13) in using Permutation and Combination is given below. If  $Q < 2$ , it is obvious that at least one end must have the direction data lost, so the probability of accurately recognizing the faulted line is 0.

If  $2 \leq Q < \delta$ , the number of events without the information on faulted line or with one specific end receiving the direction data is  $\sum_{i=0}^Q C_\delta^i C_{Q^0-2\delta}^{Q-i}$ , where  $C_\delta^i$  is to take  $i$  data from the information at specific end of the faulted line, and  $C_{Q^0-2\delta}^{Q-i}$  is to take  $Q-i$  data from the information on non-faulted line. Thus, the number of events without the information on faulted line or with either one end receiving the direction data is  $2 \sum_{i=0}^Q C_\delta^i C_{Q^0-2\delta}^{Q-i} - C_{Q^0-2\delta}^Q$ , where  $C_{Q^0-2\delta}^Q$  is the number of events without faulted line information. Because the repetition is accumulated, it needs to be subtracted from the sum. And the number of elementary events uploaded in area  $\Lambda$  and receiving  $Q$  direction data is  $C_{Q^0}^Q$ . Therefore, the probability of accurately recognizing the faulted line is  $1 - \frac{2 \sum_{i=0}^Q C_\delta^i C_{Q^0-2\delta}^{Q-i} - C_{Q^0-2\delta}^Q}{C_{Q^0}^Q}$ .

If  $\delta \leq Q \leq Q^0 - 2\delta$ , as in previous analysis, it is concluded that the probability of accurately recognizing the faulted line is  $1 - \frac{2 \sum_{i=0}^\delta C_\delta^i C_{Q^0-2\delta}^{Q-i} - C_{Q^0-2\delta}^Q}{C_{Q^0}^Q}$ . If  $Q^0 - 2\delta < Q \leq Q^0 - \delta$ , the number of events that can receive the direction data of one end but not both ends is  $2 \sum_{i=\beta}^\delta C_\delta^i C_{Q^0-2\delta}^{Q-i}$ . And the number of elementary events uploaded in area  $\Lambda$  and receiving  $Q$  direction data also is  $C_{Q^0}^Q$ . Therefore, the probability of accurately recognizing the faulted line is  $1 - \frac{2 \sum_{i=\beta}^\delta C_\delta^i C_{Q^0-2\delta}^{Q-i}}{C_{Q^0}^Q}$ . Then  $Q^0 - \delta < Q \leq Q^0$ ; it is apparent that the direction angle data at both ends of the faulted line must be received; so the probability of accurately recognizing the faulted line is 1.

### D. Reliability of Whole Decision Process in WAPS

The WAPS for decision-making process is reliable only when the three proposed modules perform reliably. The accuracy of WAPS decision at the control center can be expressed as

$$P_{ctr} = P_{sf} P_{fz} P_{fl} \quad (14)$$

In particular, when it satisfies:

$$\begin{cases} S > \max\{S^0 - \gamma\delta + 1, S^0 - \alpha\delta + 1\} \\ Q > Q^0 - \delta \end{cases} \quad (15)$$

there is  $P_{ctr} = 1$ .

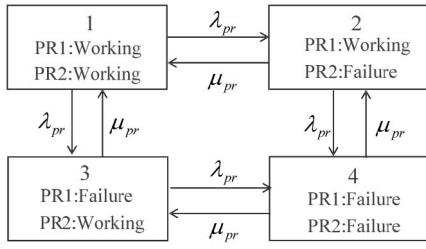


Fig. 4. State transition of two protection IEDs in a substation.

#### IV. WAPS RELIABILITY INDICES AND ANALYSES METHOD

##### A. WAPS Function Process at Substations

When the control center submits a trip command, the fault isolation will occur only when protection IEDs in corresponding substations can function accordingly. In order to highlight the focus of the paper on the wide-area model, it is considered that the data transmission process in the substation LAN is reliable and protection IEDs have redundant configurations. Suppose that the failure rate of the protection IEDs is  $\lambda_{pr}$  and the repair rate is  $\mu_{pr}$ . The dual state transition for protection IEDs is shown in Fig. 4.

Using the solution of the Markov model, the probability of normal operation of substation protection IEDs at steady state is presented as

$$p_{pro} = 1 - \frac{\lambda_{pr}^2}{(\lambda_{pr} + \mu_{pr})^2}. \quad (16)$$

##### B. Definitions of WAPS Reliability Indices

WAPS reliability indices are defined as: average decision accuracy  $P_{ctr}$ , average operation accuracy  $P_{act}$ , and mean available time  $MAT$ .

Suppose there are  $k_T$  WAN states; the average accuracy of WAPS decision-making process is stated as

$$P_{ctr} = \frac{\sum_{i=1}^{k_T} P_{ctr}^i}{k_T} \quad (17)$$

Then, the average operation accuracy of WAPS is derived by (6).

Assume the WAPS is considered reliable if the probability of identifying and isolating the fault correctly is more than 90%; otherwise WAPS is considered unreliable. Thus, the mean available time of WAPS is defined as

$$MAT = \frac{1}{b_{01}} \quad (18)$$

where  $b_{01}$  is the WAPS transition rate from available to unavailable states.

##### C. WAPS Procedure for Reliability Index Computation

The complex network topology and large numbers of WAPS components result in an enormous state space, which makes it difficult to calculate the reliability indices using analytical methods. We apply a sequential Monte-Carlo simulation method to calculate the WAPS reliability indices in this paper.

Components in cyber space adopt a composite Markov model for their coupling with the physical layer in CPPS, whereby the maximum flow is obtained by a linear programming model [22].

The specific steps for the computation of WAPS reliability indices are stated as follows:

1. Initialize the  $N_c$  component states and the simulation time. For a two-state component, its initial state is set to in operation. For a multi-state component, its initial state is set to that of the largest capacity. The simulation time is initialized to  $t = 0$ ; the sojourn time and the number of times of system availability are initialized to  $t_s = 0$  and  $k_s = 0$ ; the sojourn time and the number of times of system unavailability are initialized to  $t_f = 0$  and  $k_f = 0$ , respectively.

2. Sample the component duration by extracting a random number  $rand$  from the uniform distribution  $U(0, 1)$ ; the sojourn time of component  $i$  in the current state is  $t_i = -\bar{T}_i \ln(rand)$ , and  $\bar{T}_i$  is the mean sojourn time of the component in the current state.

3. Calculate and update the system duration  $t_{dur}$  in the current state. The current state duration depends on the component with the shortest duration. There is  $t_{dur} = \min\{t_i; 1 \leq i \leq N_c\}$ . Update the system simulation time  $t = t + t_{dur}$ . The duration of each component is updated to  $t_i = t_i - t_{dur}$ .

4. Solve the network flow model of WAN to acquire the data acceptance rate  $d$  in the current system state. Furthermore, calculate the accuracy of WAPS decision process for  $d$  according to (14). If the accuracy exceeds 90% and in the current state of the protection IEDs in the substation is in the operation state, the current system state is reliable. Then update the sojourn time  $t_s = t_s + t_{dur}$  and the cumulative number of reliable operations ( $k_s = k_s + 1$ ). Otherwise, update the sojourn time  $t_f = t_f + t_{dur}$  and the cumulative number of unavailable operations ( $k_f = k_f + 1$ ).

5. Update component and system states, and repeat Step 3.

6. Stop the iterative process if the coefficient of variation of all reliability indices satisfies the convergence condition determined by (19) during the simulation process [23].

$$\frac{\sqrt{V(R)}/K_{sim}}{E(R)} \leq \varepsilon \quad (19)$$

where  $R$  represents the reliability index;  $V(R)$  is the variance of  $R$ ;  $E(R)$  is the mean value of  $R$ .  $K_{sim}$  is the number of updates of system state; and  $\varepsilon$  is a preset value which is very small.

Finally, the unbiased estimation of the expected value of the mean available time is calculated by the Monte-Carlo simulation as follows:

$$\widetilde{MAT} = \frac{t_s}{k_s}. \quad (20)$$

#### V. CASE STUDY

##### A. Case Description

In this paper, the reliability of the WAPS is analyzed when a line fault occurs in the IEEE 14-bus system. There are 14 nodes and 20 branches in the power system, among which Nodes 5 and 6 belong to one substation, Nodes 4, 7, 8, and 9 belong to another substation, resulting in a 10-node

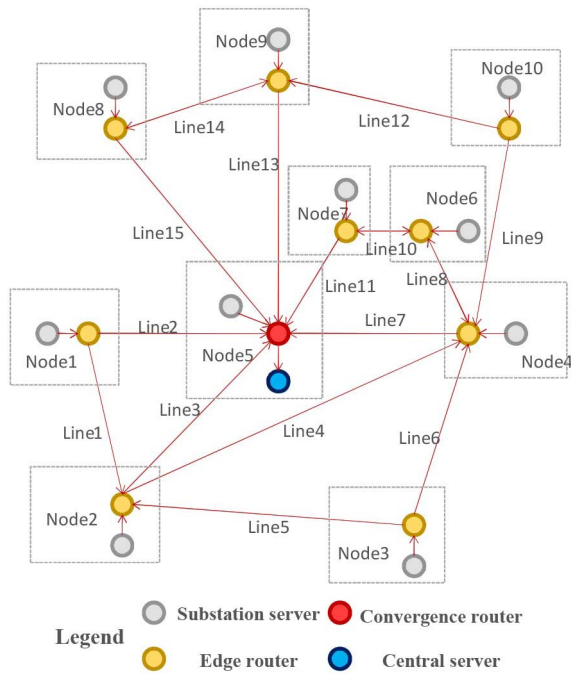


Fig. 5. Wide-area communication network constructed in the IEEE 14-bus system.

and 15-link model in the communication system [24]. The communication links are generally erected in parallel with transmission lines. Therefore, the communication network topology is similar to that of the power grid.

In order to focus on the WAPS reliability, substation LAN communication devices (such as switches) are considered reliable. The substation servers for WAMS data collection are abstracted into data source nodes, and routers are abstracted into routing nodes. Node 5 in the regional master station where the control center performs WAPS calculations. The substation servers upload data through edge routers, and the convergence router in the master station collects the data uploaded by each substation to the central server of the control center. Synchronous digital hierarchy (SDH) optical fiber communication is adopted in the overall architecture. Synchronous Transport Module level-1 (STM-1) mode is used to connect the nodes, all routers support full-duplex communication, and transmission rate is 155Mb/s. In order to cope with the N-1 principle, we assume there are at least two upload paths from each substation. The wide-area communication network based on the IEEE 14-bus system is shown in Fig. 5. The substation is abstracted as a single node, which contains a substation server uploaded data and redundant configuration protection IEDs undertaking the tripping function.

For the same communication network layout in the IEEE 14-bus system, with an increase in capacity or decrease in demand, the system reliability will be determined by not only the blockage of information flow but also physical system failures [22]. Therefore, it is necessary to model WAPS with CPPS constraints. The substation server adopts a composite Markov model and other components use a two-state Markov model. In order to highlight the influence of limited

TABLE I  
ALLOCATION OF COMPONENT  $i^{\text{th}}$  IN EACH STATE OF SUB-SERVER

Physical State	Cyber State No.	Capacity (Mb/s)	Steady-state Probability without physical failure	Steady-state Probability with physical failure
Operation	1	15	70%	69.9790%
	2	20	15%	14.9955%
	3	25	10%	9.9970%
	4	30	5%	4.9985%
Failure	0	0	0.03%	

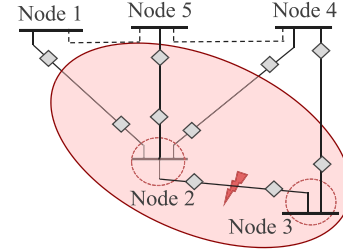


Fig. 6. Schematic of the fault area.

information flow, we set the information system traffic at a higher level, while the failure rate of physical equipment is rather lower. The steady-state probability distribution of each substation server is solved by the statistical sample data shown in Table I. We further make the following assumptions. The failure rate of the routers is  $0.02\text{year}^{-1}$ . When a router is in operation state, its constrained capacity is 155 Mb/s. The failure rate of the central server is  $0.01\text{year}^{-1}$  which has sufficient bandwidth; thus, there is no need to set a capacity constraint. The failure rate of protection IEDs is  $0.0067\text{year}^{-1}$ . The component repair time is 24h.

Assume that a short-circuit fault occurs near the middle of Line 5 between Nodes 2 and 3, and the positive sequence voltage of Nodes 2 and 3 is lower than that of initiation setting value. Then the fault area consists of Nodes 2, 3 and all respective lines. Here,  $\Upsilon = 2$  and  $\alpha = 2$ . The directional element is provided at sending and receiving ends of each line. The total number of directional elements in the fault area is  $2\text{card}(L) = 10$  as shown in Fig. 6. Among all reliability indices, it can be seen by calculating (19) that the variance coefficient of  $MAT$  has the slowest convergence rate. Therefore, the variance coefficient of  $MAT$  index is adopted as the criterion for the convergence of simulation; Also,  $\varepsilon$  is set at  $10^{-5}$ .

## B. Reliability Index Calculation Results and Analyses

1) *Impact of Data Performance on WAPS Reliability:* We consider several scenarios with different network bandwidth levels and data redundancy uploaded by each substation. The data acceptance rate of WAN, the operation accuracy of WAPS, and mean available time of WAPS corresponding to data redundancy in various scenarios are shown in Figs. 7–9. The curves show reliability indices for varying data redundancy and network bandwidth. It is shown that with different bandwidth configurations, the data acceptance rate at the control center is reduced, WAPS operation accuracy is decreased,

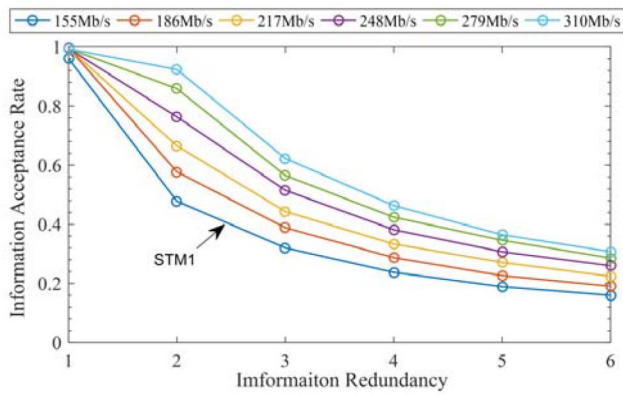


Fig. 7. Information acceptance rate corresponding to WAN in different scenarios.

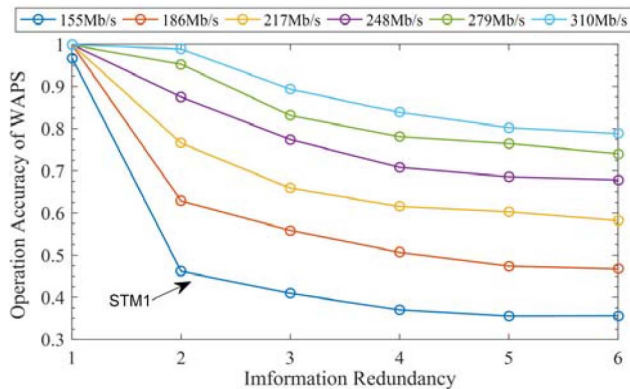


Fig. 8. Operation accuracy of WAPS in different scenarios.

and *MAT* takes a downward trend, as the data redundancy is increased. In this case, the maximum operation accuracy of WAPS occurs when the data redundancy is 1, irrespective of the bandwidth configuration in scenarios.

With respect to WAPS decisions, any loss of critical fault data will lead to a failure in the protection decision and reduce the operation accuracy of WAPS because there is no redundancy in data. However, with respect to WAN, because the data redundancy is the lowest in this case, the network bandwidth is quite sufficient and the data acceptance rate at the control center is almost 100%, which means that the control center can completely retrieve all the data. Therefore, WAPS has the highest operation accuracy, when the data redundancy is 1.

As the network bandwidth increases, the WAPS operation accuracy corresponding to the different data redundancy will increase differently. In particular, when the bandwidth is upgraded from 155Mb/s to 310Mb/s, and the information redundancy is increased from 1 to 2, the WAPS operation accuracy jumps from 45% to 98%. Also, using the 310Mb/s bandwidth, the WAPS decision process can work reliably, because it only needs to receive any one copy of data, although the data acceptance rate is only about 95%. So, the WAPS accuracy has not been affected as compared to the case when the redundancy was 1. For STM1 scenario, when the data redundancy is increased to 2, the data acceptance

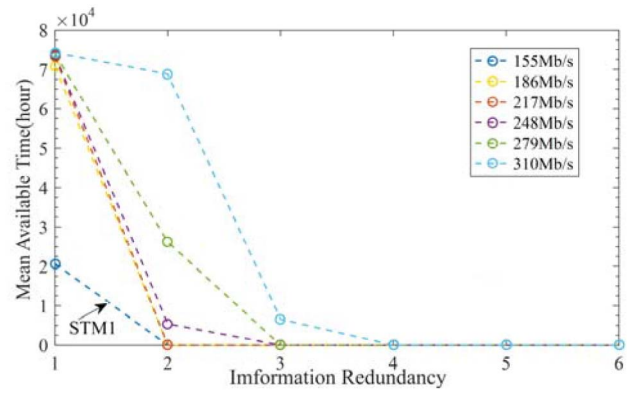


Fig. 9. Mean available time of WAPS in different scenarios.

rate drops rapidly to 47%, which indicates that the network congestion would be troublesome. Accordingly, WAPS will receive an insufficient level of data for fault recognition and the protection accuracy would be very low in this scenario.

It can be found that the mean available time of WAPS is leveled off faster by increasing the data redundancy than the operation accuracy of protection. This is because when the bandwidth is not high enough, the WAN performance tends to be saturated with a higher level of data redundancy. The data acceptance rate will drop rapidly, which eventually results in lowering the accuracy below 90%. Once the WAPS operation accuracy drops to 90%, the *MAT* of the system is levelled-off to 0. In particular, when the data redundancy reaches 4, the *MAT* of WAPS is levelled-off to 0 for various network bandwidth configurations. This indicates that when the data redundancy reaches 4, adopting the bandwidth below 310Mb/s inevitably cannot meet the conditions that the WAPS operation accuracy reaches 90%.

Obviously, improving the data redundancy is beneficial to the power system operations. However, the WAN bandwidth is limited and increasing the data redundancy would indefinitely aggravates the WAN burden. Accordingly, a large sum of distributed data may not be utilized effectively by the control center which would deteriorate the power system performance. Therefore, only when the data redundancy increases properly with sufficient bandwidth, can the richness of additional data be enlightened in the control center and can the WAPS operation accuracy and the system availability be enhanced further.

2) *Impact of Grid Topology on WAPS Reliability*: Suppose that a fault occurs on each power line separately, the network bandwidth configuration is set to 310Mb/s, and the data redundancy uploaded by each substation is set to 3. In this arrangement, the WAPS operation accuracy is shown in Fig. 10. Here, when the network performance is determined, there is little difference in the WAPS operation accuracy between power lines. The difference between the line with the highest operation accuracy and that with the lowest one is only within 5%.

This small difference is limited by the power grid topology, because the resulting fault area is different when the faults occur on different lines, which is due to the number of outgoing lines from each grid node. Under normal circumstances,

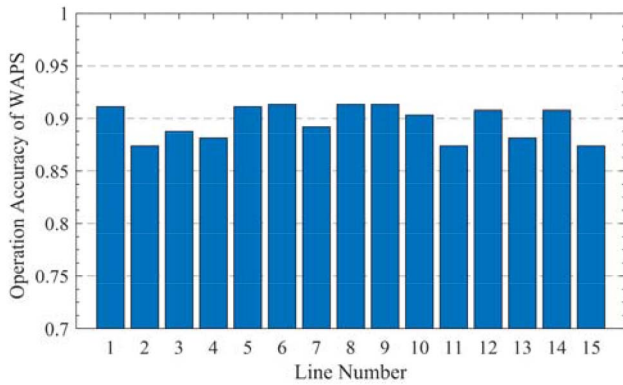


Fig. 10. WAPS operation accuracy for different transmission line faults.

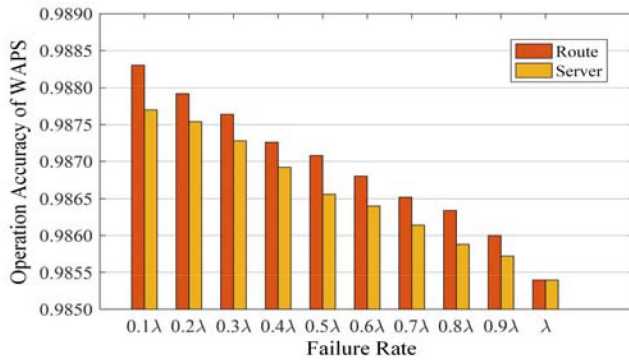


Fig. 11. Impact of WAN failure rate on WAPS operation accuracy.

the initiation module is rather sensitive and, therefore, the difference in the accuracy of the initiation module in the case of single line fault will be minimal. As the fault area positioning module works similar to the initiation module, even if the sequence voltage data of the bus associated with a non-faulty line is lost, it will not result in a positioning failure. Also, the accuracy of the faulted line recognition module is close in different cases, because there is little difference in the number of outgoing lines in different line faults. That is, the topology of the regional power grid has a minute effect on the WAPS reliability.

3) *Impact of Failure Rate on WAPS Reliability*: Suppose that a fault occurs on Line 5 between Nodes 2 and 3, the network bandwidth configuration is set to 310Mb/s, and the redundancy of the data uploaded by each node is set to 2. Then, the impact of changing the failure rate of WAN on the WAPS operation accuracy is shown in Fig. 11. Obviously, as the failure rate of WAN decreases, the WAPS operation accuracy will gradually improve, but the extent of improvement is very poor. Even if the failure rate is reduced to one tenth of the initial setting value, the WAPS operation accuracy is only improved by less than 0.3%. Reducing the equipment failure rate would require the adoption of better materials and technologies, which means investing a lot of manpower and financial resources, which may only have a little effect on the WAPS reliability enhancement.

In summary, the most serious factor which influences the WAPS reliability is the performance of cyber layer, while

the power grid topology and the WAN failure rate will have a minute influence on the WAPS reliability. Because the core of WAPS includes the decision-making process, the WAPS decision to accurately identify and isolate the faulted element will depend on the amount of data received by the control center and the state of cyber layer.

The impact of the WAN equipment failure rate on its network performance will only be apparent when the equipment is placed out of service. Generally, the failure duration and frequency are relatively low, so even if the WAN failure rate is further reduced, its network performance cannot be improved, and the amount of data received by the control center is insufficient. Any upgrading of network bandwidth can directly improve the performance of the cyber space and make the control center have a higher data acceptance rate when facing large traffic pressure, substantially improve the accuracy of wide-area decision-making, and thus ensure a high reliability level of the WAPS.

So, when the regional power grid needs to be equipped with WAPS, it should give priority to ensure the adequacy of wide-area communication network performance. On this basis, it can further improve the data redundancy and the quality of equipment to improve reliability.

## VI. CONCLUSION

The emerging networked protection system is highly sensitive to information performance. It needs to go deep into the information level for quantitative modeling and analysis. This paper makes an exploration on the reliability modeling of wide-area protection system. The decision-making accuracy of the wide-area protection algorithm is proposed by building the relationship between algorithms and limited information. In addition, the operation accuracy of the wide-area protection and the tripping reliability of the corresponding substation protection device are enhanced. Consequently, a complete reliability analysis model is established considering cyber-physical system constraints, and the importance of wide-area information flow to the reliability of WAPS is verified by an example. If the adequacy of WAN bandwidth cannot be guaranteed, any increase in data redundancy would not effectively improve the decision accuracy of the protection algorithm. In this case, the power grid topology and the failure rate of communication equipment have a minute impact on the WAPS reliability. The proposed modeling method combined deeply with the information flow level and the protection algorithm expands the traditional reliability assessment method which considers the system function failure caused by mechanical problems of devices at the physical level. The proposed reliability analysis methodology, which combines a series of innovative ideas and research methods organically, also provides a new idea concerning the reliability evaluation of the coupled cyber-physical systems regarded WAPS as a middleware in smart grid.

## REFERENCES

- [1] B. Falahati, Y. Fu, and L. Wu, "Reliability assessment of smart grid considering direct cyber-power interdependencies," *IEEE Trans. Smart Grid*, vol. 3, no. 3, pp. 1515–1524, Sep. 2012.

- [2] A. Vafamehr and M. E. Khodayar, "Expansion planning of data centers in energy and cyber networks," in *Proc. IEEE Power Energy Soc. Gen. Meeting*, Jul. 2016, pp. 1–5.
- [3] J. De La Ree, V. Centeno, J. S. Thorp, and A. G. Phadke, "Synchronized phasor measurement applications in power systems," *IEEE Trans. Smart Grid*, vol. 1, no. 1, pp. 20–27, Jun. 2010.
- [4] J. Bertsch, C. Carnal, D. Karlson, J. McDaniel, and K. Vu, "Wide-area protection and power system utilization," *Proc. IEEE*, vol. 93, no. 5, pp. 997–1003, May 2005.
- [5] M. K. Jena, S. R. Samantaray, and B. K. Panigrahi, "A new decentralized approach to wide-area back-up protection of transmission lines," *IEEE Syst. J.*, vol. 12, no. 4, pp. 3161–3168, Dec. 2018.
- [6] X. Tong, X. Wang, and K. M. Hopkinson, "The modeling and verification of peer-to-peer negotiating multiagent colored Petri nets for wide-area backup protection," *IEEE Trans. Power Del.*, vol. 24, no. 1, pp. 61–72, Jan. 2009.
- [7] M. M. Eissa, "A novel centralized wide area protection 'CWAP' in phase portrait based on pilot wire including phase comparison," *IEEE Trans. Smart Grid*, vol. 10, no. 3, pp. 2671–2682, May 2019.
- [8] "Back-up protection and overall protection of power system networks SC 34 ELT\_034\_5," *Electra Session Papers, CIGRE*, Paris, France, Rep. 1974, Aug. 2017.
- [9] Y. Serizawa *et al.*, "Wide-area current differential backup protection employing broadband communications and time transfer systems," *IEEE Trans. Power Del.*, vol. 13, no. 4, pp. 1046–1052, Oct. 1998.
- [10] K. Kangvansaichol and P. A. Crossley, "Multi-zone differential protection for transmission networks," in *Proc. Inst. Elect. Eng. Develop. Power Syst. Protect. Conf.*, vol. 2. Amsterdam, The Netherlands, 2004, pp. 428–431.
- [11] X. Lin, Z. Li, K. Wu, and H. Weng, "Principles and implementations of hierarchical region defensive systems of power grid," *IEEE Trans. Power Del.*, vol. 24, no. 1, pp. 30–37, Jan. 2009.
- [12] Z. He, Z. Zhang, W. Chen, O. P. Malik, and X. Yin, "Wide-area backup protection algorithm based on fault component voltage distribution," *IEEE Trans. Power Del.*, vol. 26, no. 4, pp. 2752–2760, Oct. 2011.
- [13] Z. L. Yang, D. Y. Shi, and X. Z. Duan, "Wide-area protection system based on direction comparison principle," *Proc. Chin. Soc. Electr. Electron. Eng.*, vol. 28, no. 22, pp. 87–93, Aug. 2008.
- [14] Z.-H. Dai, Z.-P. Wang, and Y.-J. Jiao, "Reliability evaluation of the communication network in wide-area protection," *IEEE Trans. Power Del.*, vol. 26, no. 4, pp. 2523–2530, Oct. 2011.
- [15] Y. Wang, W. Li, and J. Lu, "Reliability analysis of wide-area measurement system," *IEEE Trans. Power Del.*, vol. 25, no. 3, pp. 1483–1491, Jul. 2010.
- [16] W. Liu, Q. Gong, H. Han, Z. Wang, and L. Wang, "Reliability modeling and evaluation of active cyber physical distribution system," *IEEE Trans. Power Syst.*, vol. 33, no. 6, pp. 7096–7108, Nov. 2018.
- [17] J. Duan, H. Xu, and W. Liu, "Q-learning-based damping control of wide-area power systems under cyber uncertainties," *IEEE Trans. Smart Grid*, vol. 9, no. 6, pp. 6408–6418, Nov. 2018.
- [18] Q. Zhou, M. Shahidehpour, A. Paaso, S. Bahramirad, A. Abdulwahab, and A. M. Abusorrah, "Distributed control and communication strategies in networked microgrids," *IEEE Commun. Surveys Tuts.*, vol. 22, no. 4, pp. 2586–2633, 4th Quart., 2020, doi: [10.1109/COMST.2020.3023963](https://doi.org/10.1109/COMST.2020.3023963).
- [19] J. Zare, F. Aminifar, and M. Sanaye-Pasand, "Communication-constrained regionalization of power systems for synchrophasor-based wide-area backup protection scheme," *IEEE Trans. Smart Grid*, vol. 6, no. 3, pp. 1530–1538, May 2015.
- [20] R. He, H. Peng, Q. Jiang, L. Zhou, and J. Zhu, "Performance analysis and threshold quantization of transformer differential protection under sampled value packets loss/delay," *IEEE Access*, vol. 7, pp. 55698–55706, 2019.
- [21] R. He, J. Deng, and L. L. Lai, "Reliability evaluation of communication-constrained protection systems using stochastic-flow network models," *IEEE Trans. Smart Grid*, vol. 9, no. 3, pp. 2371–2381, May 2018.
- [22] R. He, H. Xie, J. Deng, T. Feng, L. L. Lai, and M. Shahidehpour, "Reliability modeling and assessment of cyber space in cyber-physical power system," *IEEE Trans. Smart Grid*, vol. 11, no. 5, pp. 3763–3773, Sep. 2020.
- [23] A. Sankar Krishnan and R. Billinton, "Sequential Monte Carlo simulation for composite power system reliability analysis with time varying loads," *IEEE Trans. Power Syst.*, vol. 10, no. 3, pp. 1540–1545, Aug. 1995.
- [24] R. Giovanini, K. Hopkinson, D. V. Coury, and J. S. Thorp, "A primary and backup cooperative protection system based on wide area agents," *IEEE Trans. Power Del.*, vol. 21, no. 3, pp. 1222–1230, Jul. 2006.



**Ruiwen He** (Senior Member, IEEE) received the B.E. degree in machine engineering from Zhejiang University, Hangzhou, China, in 1990, the M.S. degree in electrical engineering from Wuhan University, Wuhan, China, in 1995, and the Ph.D. degree in electrical engineering from the South China University of Technology, Guangzhou, China, in 2005.

She is currently a Full Professor with the School of Automation, Guangdong University of Technology, Guangzhou. Her current research interests are intelligent protection of power systems, IEC 61850-based substation automation systems, and cyber-physical power systems.



**Shenghui Yang** received the B.E. degree in electrical engineering from the Guangdong University of Technology, Guangzhou, China, in 2019, where he is currently pursuing the M.S. degree with the Department of Electrical Engineering, School of Automation.

His research interests include power system protection and control, and cyber-physical power systems.



**Jianhua Deng** received the B.E. degree in electrical engineering from Guangdong University, Guangzhou, China, in 2015, and the M.S. degree in electrical engineering with the School of Automation, Guangdong University of Technology, Guangzhou, in 2018.

He is currently an Engineer with the Foshan Electric Power Company Ltd. of China, Southern Power Grid, Foshan, China. His current research interests are intelligent protection of power systems, and cyber-physical power systems.



**Teng Feng** received the B.Sc. and Ph.D. degrees in electrical engineering from Tsinghua University, Beijing, China, in 2012 and 2017, respectively. He is with the Automation and Control Design Research Center, State Grid Economic and Technological Research Institute Company Ltd., Beijing. His research interests include power system protection and control, smart grid planning, and design.



**Loi Lei Lai** (Fellow, IEEE) received the B.Sc. and Ph.D. degrees from the University of Aston, Birmingham, U.K., in 1980 and 1984, respectively, and the D.Sc. degree from the City University of London, U.K., in 2015. He is currently the University Distinguished Professor with the Guangdong University of Technology, Guangzhou, China. He is a Fellow of IET and National Distinguished Expert in China, and Distinguished Expert in State Grid Corporation of China.



**Mohammad Shahidehpour** (Life Fellow, IEEE) received the Honorary Doctorate degree from the Polytechnic University of Bucharest, Bucharest, Romania. He is a University Distinguished Professor, the Bodine Chair Professor, and the Director of the Robert W. Galvin Center for Electricity Innovation, Illinois Institute of Technology. He is a member of the U.S. National Academy of Engineering. He is a Fellow of the American Association for the Advancement of Science and the National Academy of Inventors.